Soils and Rocks
An International Journal of Geotechnical and Geoenvironmental Engineering
www.soilsandrocks.com
ISSN 1980-9743
ISSN-e 2675-5475

An evaluation of reinforcement mechanical damages in geosynthetic reinforced piled embankments

Ennio Marques Palmeira[1], José Melchior Filho[1#],
Ewerton Clayton Alves Fonseca[2]

Article

Keywords
Geosynthetics
Reinforcement
Piled embankments
Mechanical damage

Abstract

The use of geosynthetic reinforcement in piled embankments over soft soils is an effective solution for the reduction of settlements and to increase the embankment stability. The most efficient position for the reinforcement layer is on the pile cap or head. However, a direct contact of the reinforcement with sharp edges may damage it, compromising its efficiency to transfer loads to the piles. This paper investigates the possibility of mechanical damages in geosynthetic reinforcements on pile caps by large scale laboratory tests. Tests with and without pieces of nonwoven geotextile protective layer between the caps and the reinforcements were executed. Wide strip tensile tests were performed on exhumed reinforcement specimens after the tests to assess tensile strength and stiffness variations. A statistical analysis of the results shows reductions in tensile strength of unprotected reinforcement layers of up to 28%. A mechanical damage index is introduced and its correlation with calculated reduction factors is investigated. The use of a piece of a thick geotextile layer to protect the reinforcement against mechanical damage can be effective. However, the geotextile product must be properly specified and installed with due care.

1 Introduction

The design of embankments on soft soils must guarantee not only the embankment stability but also that its settlements due to soft soil consolidation will not compromise its function. In this context, the use of piles to transfer the embankment load (self-weight and surcharges) to deeper strong layers can be an effective solution to minimize settlements and increase the overall stability of the embankment. The presence of the piles as rigid elements compared to the soft soil compressible nature causes arching of the fill material between the piles, yielding to the transference of loads to the piles and reduction of stresses acting on the surface of the soft subgrade. However, the solution must be properly designed to guarantee an effective mechanism of load transfer to the piles and from them to a stiffer soil layer underneath the soft soil.

The use of geosynthetic reinforcement in piled embankments has increases significantly in the last 4 decades. The reasons for this are that the presence of the geosynthetic layer improves the load transfer to the piles and reduces even further the stresses transmitted to the soft foundation soil. In addition, the reinforcement increases the safety of the embankment against global failure. However, the interaction between fill material, reinforcement and piles is complex and different analytical and numerical studies can be found in the literature to address this problem (Low et al., 1994; Russel & Pierpoint, 1997; Filz & Smith, 2006; Filz & Smith, 2007; Abusharar et al., 2009; Sloan et al., 2011; Zhuang et al., 2014; van Eekelen., 2015; Fattah et al., 2015; Fattah et al., 2016a, b; Fonseca & Palmeira, 2018, Fonseca et al., 2018; Al-Taie et al., 2019). Standards and guidelines can also be found to help the design and construction of such works complying with technical requirements and appropriate safety margins (BSI, 2010; EBGEO, 2011; FHWA, 2017; van Eekelen, 2016).

Figure 1 shows the typical deformation pattern of a bottom reinforcement layer in a geosynthetic reinforced piled embankment after consolidation of the soft soil. The most efficient position for the reinforcement layer is on the pile caps or heads, when the former is not present (Fonseca

#Corresponding author: E-mail address: melchior_filho@hotmail.com
[1]Universidade de Brasília, Departamento de Engenharia Civil e Ambiental, Brasília, DF, Brasil.
[2]Universidade Federal Tecnológica do Paraná, Departamento de Construção Civil, Campo Mourão, PR, Brasil.

Submitted on January 11, 2022; Final Acceptance on May 21, 2022; Discussion open until: November 30, 2022.
https://doi.org/10.28927/SR.2022.000522

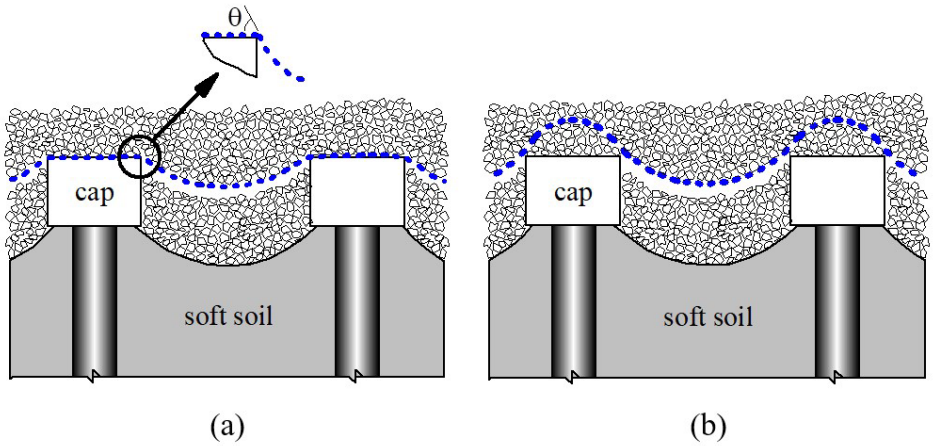

Figure 1. Typical deformation patterns of the bottom reinforcement layer in a piled embankment:S (a) reinforcement initially in contact with cap; (b) reinforcement above cap.

& Palmeira, 2018). However, this direct contact between the reinforcement and a rigid body, usually with sharp edges, defects, and lack of proper finishing, may damage the reinforcement along the edges of the cap or pile head to the point of tearing the reinforcement entirely along the cap or pile perimeter, as exemplified in Figure 2a. This damaging mechanism is particularly relevant under repeated loading, which is likely to occur during the construction of the embankment and during its operational life in embankments for highways and railways, for instance. To avoid or minimize this possibility of mechanical damage, a protective thick nonwoven geotextile layer can be installed between the reinforcement and the cap/pile, as shown in Figure 2b. However, it should be pointed out that both Figures 2a,b were from the same work. So, the torn geogrid reinforcement in Figure 2a was also protected by a geotextile layer. Therefore, due care must be taken in the specification of the protective geotextile layer and construction practice to avoid failure of the reinforcement in contact with the cap. van Eekelen (2016) recommends caps with beveled edges to avoid or minimize such damages. Some recommendations are more restrictive, stablishing that the reinforcement layer must be placed some minimum distance above the pile cap/head to avoid direct contact between them (EBGEO, 2011). Almeida & Marques (2011) recommend a 150 mm thick sand layer to be installed between the reinforcement and the pile cap. BSI (2010) also recommends a layer of sand between reinforcement and caps. It should be pointed out that even with the reinforcement above the cap (Figure 1b), some level of mechanical damage of the reinforcement should be expected due to the abrasive nature of the interaction between soil and reinforcement, particularly under repeated loading and in the long-term. Thus, appropriate reduction factors for the relevant mechanical properties of the reinforcement must be chosen to avoid problems such as those shown in Figure 2a.

Several works on geosynthetic mechanical damage can be found in the literature (Azambuja, 1994; Richardson, 1998; Hufenus et al., 2002; Huang, 2006; Bathurst & Miyata, 2015; Pinho-Lopes et al., 2018; Fleury et al., 2019, for instance). These works have investigated the intensity and/or estimate appropriate reduction factors by laboratory and field tests. Some studies involved the use of standard laboratory tests to evaluate mechanical damages to reinforcements under repeated loading (Cho at al., 2006; Yoo et al. 2009; Rosete et al., 2013; Gonzalez-Torre et al., 2014). Large scale field tests have also been performed to investigate mechanical damages of geosynthetic reinforcements (Austin, 1997; Richardson, 1998; Hsieh & Wu, 2001; Hufenus et al., 2002; Cho et al., 2006; Fleury et al., 2019). However, the authors of the present paper are not aware of any study on damage to reinforcements in piled embankments on soft soils.

Due to the relevance of the problem described above, this paper aimed at investigating the intensity and consequences of mechanical damages of reinforcements in contact with the edge of rigid bodies, such as in the case of concrete caps in piled embankments. An evaluation of the contribution of a thick nonwoven geotextile layer between the cap and the reinforcement was also investigated.

2. Experimental

2.1. Equipment

A large equipment developed for tests on large scale models of geosynthetic reinforced piled embankments (Fonseca, 2017; Melchior Filho, 2022) was used in this research. Figure 3 shows the geometrical characteristics of the equipment, which consists of a large rigid container (1000 mm × 1000 mm × 450 mm), made of steel, to confine

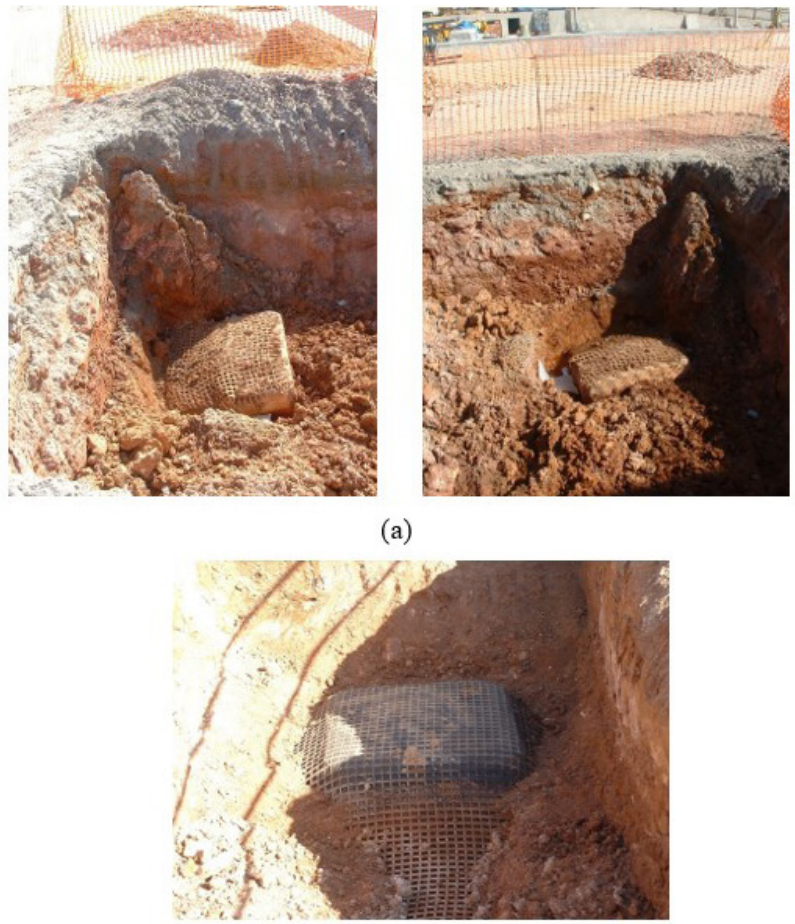

Figure 2. Example of failure of the reinforcement due to mechanical damage (a) reinforcement failure along cap perimeter; (b) protective geotextile layer between cap and geogrid reinforcement. (courtesy of Dr. Alberto Ortigão).

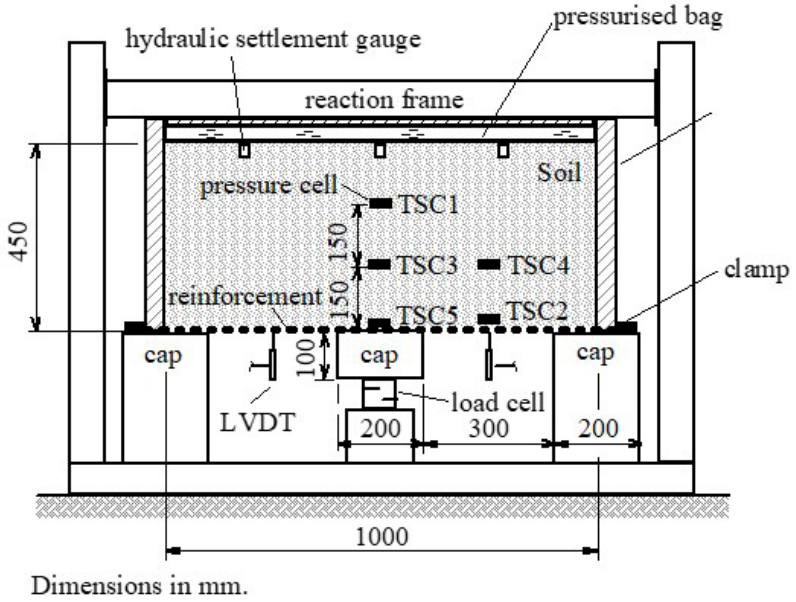

Figure 3. Equipment used in the tests.

the fill material, a reaction frame (1800 mm × 1500 mm × 1500 mm) to provide reaction to the load applied on the fill surface and a set of concrete caps (square in plan, 200 mm × 200 mm) located under the container. The spacing between centres of caps was equal to 500 mm. This spacing was chosen to simulate a typical value found under prototype conditions. The surface vertical surcharge is applied by a pressurized rubber bag that covers the entire plan area of the fill layer. The reinforcement layer is anchored along the perimeter of the container by a rigid steel clamping system. The internal walls of the container were lubricated with double layers of plastic film and grease to minimize friction with the fill layer. Tests with a single reinforcement layer and two layers at the bottom region of the fill were carried out. In all tests with a single reinforcement layer this layer was installed directly on the caps. In tests with two reinforcement layers, the bottom layer was installed directly on the caps and the upper layer was installed 50 mm above the bottom one. Figure 4a shows a general view of the equipment during one of the tests and Figure 4b shows one of the caps used in the test, which can be considered as having a much smoother and better finishing condition than those expected in the field (Figure 2a and Figure 4c). Despite having been manufactured under laboratory-controlled conditions, the caps still had defects and protrusions capable of damaging the reinforcement.

The instrumentation used in the tests consisted of a load cell to measure loads on the central pile cap, displacement transducers to measure vertical displacements of the reinforcement layer between caps, hydraulic settlement gauges to measure fill surface settlements and pressure cells distributed in the fill mass. The average reinforcement strains were obtained from measurements of movements of markers attached to the reinforcement layer. Additional information on equipment, instrumentation and testing methodology can be found in Melchior Filho (2022).

The study can be viewed as an investigation of mechanical damage of a reinforcement in contact with the edges of a rigid body in a general sense or as model scale study of a reinforced piled embankment. Considering the latter case, the dimensions of the test would simulate typical prototype conditions with a geometric scale factor (λ) ranging from 3 to 5. Hence, all the relevant typical dimensions and properties of the materials were scaled accordingly. However, as mentioned above, to some extent the tests can also simulate a prototype ($\lambda = 1$) field situation with regard to the possibility of damage, under similar conditions, of a reinforcement in contact with a rigid body, but in this case under a smaller surcharge (40 kPa, which was the maximum surcharge applied

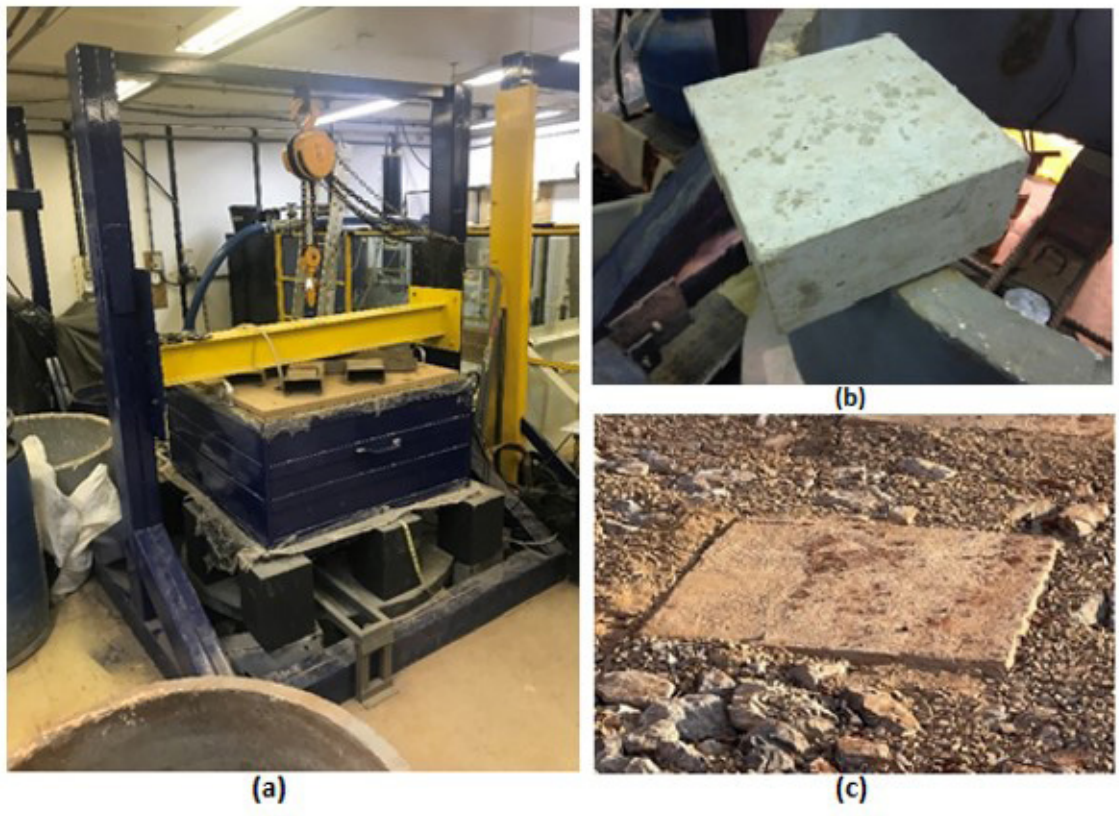

Figure 4. General view of the equipment during one of the tests performed: (a) general view; (b) view of a concrete cap; (c) typical cap surface in the field.

on the top of the fill layer) and with the actual mechanical and physical properties of the materials tested.

The maximum vertical surcharge applied on the top of the fill layer was equal to 40 kPa, which would simulate a surcharge of 200 kPa under prototype conditions in a model scale test with λ = 5. Following the stabilization of the instrumentation readings after the application of the last loading stage, the tests were disassembled, and specimens of the reinforcements were collected for tensile tests. Figure 5 depicts the locations (with respect to the cap borders) where these specimens were collected. A tensile test machine manufactured by EMIC was used in these tests, which were executed according to ASTM D4595 or ASTM D6637 (ASTM 2015, 2017), depending on the reinforcement type.

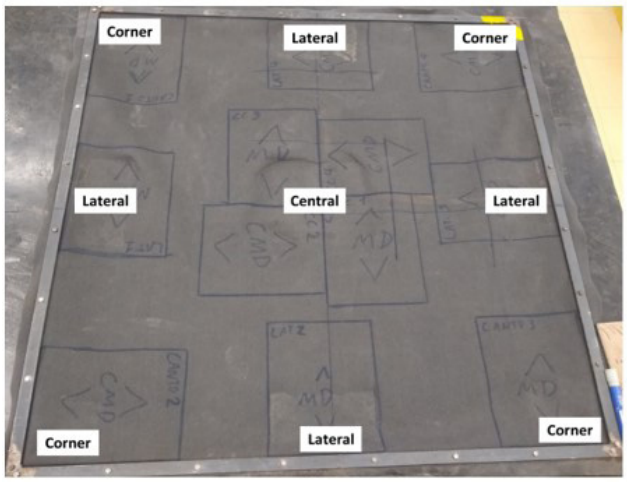

Figure 5. Locations of the specimens collected for tensile tests.

Table 1. Properties of the fill material.

ϕ' (°)(1)	43
D_{50} (mm)(2)	7.1
D_{85} (mm)(2)	10.4
C_u	2.56
γ_d (kN/m³)	16.0
I_D (%)	65
G_s(3)	2.73

Notes: (1) ϕ' = friction angle using a medium size direct shear box (300 mm × 300 mm × 175 mm), D_n = diameter for which n% of the remaining particles have smaller diameters, C_u = coefficient of uniformity (= D_{60}/D_{10}), γ_d = dry unit weight, I_D = relative density, G_s = soil particle specific gravity; (2) According to NBR 7181; (3) According to NBR 6458.

2.2 Materials

The fill material employed consisted of an uniform gravel, classified as GP according to the Unified Soil Classification System, with angular grains, an average particle diameter of 7.10 mm and a coefficient of uniformity equal to 2.56. The fill material was prepared under a loose state, with a dry unit weight of 16.0 kN/m³, yielding to a relative density of 65%. The friction angle of the fill material obtained in medium size (300 mm × 300 mm × 175 mm specimen size) direct shear tests is equal to 43°. Table 1 presents the relevant geotechnical properties of the gravel.

Six reinforcements consisting of a geogrid (code GG), a polymeric mesh (code MGR) and 4 geotextiles (codes GTX, GTA, GTB and GTC) were tested. These reinforcements were tested in the research activities carried out by Fonseca (2017) and Melchior Filho (2022). The main properties of these materials are listed in Table 2. Geogrid GG is a polyester product with square apertures, 20 mm × 20 mm wide, and a tensile stiffness at 5% strain ($J_{5\%}$) equal to 280 kN/m and 152 kN/m along machine (MD) and cross-machine (CMD) directions, respectively. The polymeric mesh (code MGR) is made of polyester, with square apertures 4 mm wide and $J_{5\%}$ of 80.2 kN/m along MD and 59.1 kN/m along CMD. Geotextiles GTX and GTA are nonwoven, needle-punched, geotextiles, made from polypropylene, with masses per unit are of 400 g/m² and 300 g/m², respectively. Reinforcements GTB and GTC are polymeric materials, made from polyester, similar to woven geotextiles, with masses per unit area equal to 75 g/m² and 185 g/m², respectively. In a real piled embankment, nonwoven geotextiles would not be suitable reinforcements due to their low tensile strength and stiffness in comparison with available geogrids and woven geotextiles. However, they were used in the present work to simulate reinforcements that would present typical mechanical properties commonly found under prototype conditions of piled embankments on soft soils, as well as to cover a wide range of reinforcement mechanical properties. Table 3 summarizes the types of tests that were performed. Duplicates of tests were carried out to assess the repeatability of the results obtained.

Table 2. Relevant properties of the geosynthetic reinforcements.

Polymer	GG	MGR	GTX	GTA	GTB	GTC
	PET	PE	PP	PP	PET	PET
M_A (g/m²)	NA	130	400	300	75	185
Aperture (mm)	20 × 20	4 × 4	NA	NA	NA	NA
T_{max} (kN/m)	17.2/10.5	13.76/13.54	18.19/18.08	15.6	5.6/5.1	10.1/6.0
ε_{max} (%)	6.4/7.1	21.0/28.3	86.1/102.5	67	71.1/53.7	9.6/13.2
$J_{5\%}$ (kN/m)	280/152	80.2/59.1	31.5/23.8	29	38/29	113/65

Notes: Results from wide-strip tensile tests as per ASTM D4595 (ASTM, 2017) or D6637 (ASTM, 2015), depending on the reinforcement considered; Numbers on the left of the slash are values along the machine direction, whereas numbers on the right are values along the cross-machine direction; NA = not applicable or not available.

Table 3. Types of tests carried out.

Test code	Reinforcement	No. of reinforcement layers	Test description
GTX-1	GTX	1	Test with one layer of GTX.
GTX-1 (R)		1	Repetition of test GTX-1.
GTX-2		2	Test with two layers of GTX.
GTX-2 (R)		2	Repetition of test GTX-2.
MGR-1	MGR	1	Test with one layer of MGR.
MGR-2		2	Test with two layers of MGR.
MGR-1 (P1)		1	Test with one layer of MGR and a protective geotextile layer with M_A = 450 g/m^2.
MGR-1 (P2)		1	Test with one layer of MGR and a protective geotextile layer with M_A = 900 g/m^2.
GG-1	GG	1	Test with one layer of GG.
GTA-1	GTA	1	Test with one layer of GTA.
GTB-1	GTB	1	Test with one layer of GTB.
GTC-1	GTC	1	Test with one layer of GTC.

Notes: M_A = mass per unit area.

If a geometrical scale factor of 5 is assumed, the reinforcements will present tensile stiffness values ranging from 725 kN/m to 7000 kN/m along machine direction and from 595 kN/m to 3800 kN/m along cross-machine direction under prototype conditions. With respect to tensile strength, under the same scale factor, the ranges would be 132 kN/m to 455 kN/m along machine direction and 128 kN/m to 452 kN/m along cross-machine direction. Values 64% smaller for the ranges above are obtained if a geometrical scale factor (λ) of 3 is considered (scale factor equal to λ^2 for reinforcement tensile strength and stiffness). If the tests are viewed as simulations of full-size problems of contact between different reinforcements and a rigid body, the properties of the reinforcement to be considered would be those in Table 2. In this case, the stress level expected on the reinforcement due to the maximum surface surcharge of 40 kPa plus the fill self-weight would be equivalent to that caused by an embankment approximately 2.9 m high. However, under such assumption only reinforcements GG, GTX, and GTA should be considered, for being actual geosynthetics, although the latter two are nonwoven products. The other reinforcements (MGR, GTB and GTC) would be too weak and extensible for most situations in practice and were tested in the current study only to attend modelling requirements in case the experiment is viewed as a model study.

Some testes were carried out with a geotextile protective layer between the reinforcement MGR and the concrete pile cap. In these tests, nonwoven, needle-punched geotextiles, made of polyester, with masses per unit area of 450 g/m^2 and 900 g/m^2 were employed as protective layers.

As mentioned before, after the tests, exhumed specimens of the reinforcements were subjected to wide-strip tensile tests and a statistical analysis (Student's *t* Test) was carried out based on results under virgin and damaged conditions to evaluate possible changes in reinforcement tensile properties with a level of confidence of 95%. Based on these analyses, reduction factors (RF) for the damage mechanisms simulated were estimated.

3. Results and discussions

3.1 Effect of mechanical damage on reinforcement tensile strength

Table 4 presents mean values of reinforcement tensile strength (T_{max}) of specimens collected at different locations (see Figure 5) after the tests. Some variations in tensile strength with respect to the strength of virgin reinforcements (Table 2) can be observed due to mechanical damages. Figure 6 shows images of reinforcements after some of the tests, where points of reinforcement distresses along the edges of the caps can be observed.

Table 5 shows the results of statistical significance if the mean values of all specimens (virgin and damaged) are compared. A statistically significant variation of T_{max} along the cross-machine direction can be observed for all tests without the protective layer of geotextile beneath the reinforcement, except for tests GTA-1 and GG-1. No statistically significant variations were observed for tests on GTX along the machine direction. On the other hand, without the presence of the geotextile protection layer, there was statistically significant variations in the tensile strength of reinforcement MGR in both directions, independent on the number of reinforcement layers present. The bottom reinforcement layer in test MGR-2 (test with 2 reinforcement layers) presented significant variation in its tensile strength, suggesting that the presence of the additional layer 50 mm above did not significantly influence the mechanical damages to the bottom layer for the conditions of the tests. It should be pointed out that the

Table 4. Tensile strength after the tests.

Test	Location (see Figure 5)	T_{max} (kN/m)		Test	Location (see Figure 5)	T_{max} (kN/m)	
		MD	CMD			MD	CMD
GTX-1	Central	14.76	20.79	MGR-1	Central	9.03	10.12
	Lateral	14.59	20.95		Lateral	10.38	11.43
	Corner	14.33	21.09		Corner	13.28	12.24
GTX-1 (R)	Central	17.10	21.55	MGR-2	Central	9.37	12.93
	Lateral	17.45	20.38		Lateral	9.74	12.08
	Corner	19.87	20.80		Corner	10.23	12.53
GTX-2	Central	17.58	20.42	MGR-1 (P1)	Central	13.46	13.69
	Lateral	16.93	21.44		Lateral	12.76	12.63
	Corner	15.67	23.05		Corner	12.22	13.11
GTX-2 (R)	Central	18.96	18.42	MGR-1 (P2)	Central	12.10	13.48
	Lateral	20.85	21.44		Lateral	13.04	12.52
	Corner	20.49	23.05		Corner	12.18	13.10

Notes: T_{max} = tensile strength after the test from wide-strip tensile tests (ASTM 2017); For exact location of specimens see Figure 5; Values of tensile strengths are mean values at each specimen location.

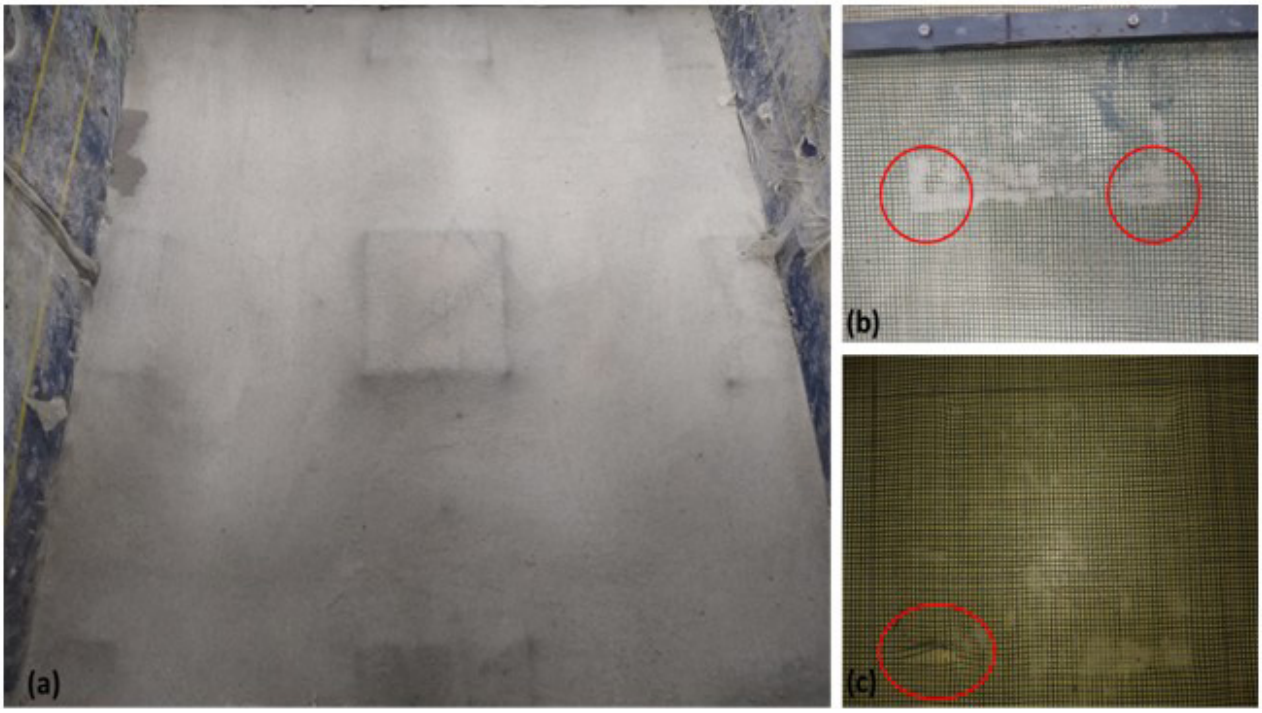

Figure 6. Images of some reinforcements at the end of the tests: (a) View of the central cap and the deformed reinforcement; (b), (c) Local damages in reinforcement.

maximum vertical displacements between caps in test MGR-2 were only 6% (along MD) and 12% (along CMD) smaller than those measured in test MGR1, for which the variations in tensile strength were also statistically significant (Table 5).

The results for tests on MGR protected with geotextile layer in Table 5 (tests MGR-1 (P1) and MGR-1 (P2)) presented no statistically significant differences, even for the lighter (M_A = 450 g/m^2) protective geotextile, showing that the nonwoven geotextile layer used was effective in minimizing the effects of mechanical damage on reinforcement tensile strength.

3.2 Effect of mechanical damage on reinforcement tensile stiffness

Table 6 presents the mean results of reinforcement tensile stiffness ($J_{5\%}$) at the end of the test at different locations, whereas Table 7 shows the statistical significance of the variations in results. Unfortunately, $J_{5\%}$ values at the end of the test are not available for reinforcements GG, GTA, GTB and GCT. In practice, variations of reinforcement tensile stiffness will increase the settlement of the base of the embankment between caps. In ten out of twelve cases

Table 5. Statistical significance of tensile strength variation.

Test	Direction	$T_{max\text{-}v}$ (kN/m)	T_{max} (kN/m)	Significance
GTX-1	MD	18.19	14.56	NS
	CMD	18.08	20.94	S
GTX-1 (R)	MD	18.19	18.14	NS
	CMD	18.08	20.91	S
GTX-2	MD	18.19	16.73	NS
	CMD	18.08	21.08	S
GTX-2 (R)	MD	18.19	20.10	NS
	CMD	18.08	20.97	S
MGR-1	MD	13.76	10.90	S
	CMD	13.54	11.26	S
MGR-2	MD	13.76	9.78	S
	CMD	13.54	12.51	S
MGR-1 (P1)	MD	13.76	12.81	NS
	CMD	13.54	13.14	NS
MGR-1 (P2)	MD	13.76	12.77	NS
	CMD	13.54	13.03	NS
GG-1	MD	15.43	15.73	NS
	CMD	8.88	8.70	NS
GTA-1	MD	14.10	13.28	NS
	CMD	19.78	19.28	NS
GTB-1	MD	6.00	3.78	S
	CMD	5.02	2.88	S
GTC-1	MD	10.38	9.96	S
	CMD	6.44	6.80	S

Notes: $T_{max\text{-}v}$ = virgin tensile strength from wide-strip tensile tests; T_{max} = tensile strength after the test from wide-strip tensile tests; MD = machine direction; CMD = cross-machine direction; NS = not statistically significant with 95% confidence level; S = statistically significant with 95% confidence level.

Table 6. Tensile stiffness ($J_{5\%}$) at different locations after the test.

Test	Location	$J_{5\%}$ (kN/m)		Test	Location	$J_{5\%}$ (kN/m)	
		MD	CMD			MD	CMD
GTX-1	Central	30.92	32.47	MGR-1	Central	63.73	53.92
	Lateral	32.74	34.45		Lateral	68.89	52.23
	Corner	27.25	23.35		Corner	66.90	50.84
GTX-1 (R)	Central	34.67	25.21	MGR-2	Central	65.80	51.99
	Lateral	30.09	21.66		Lateral	60.41	46.85
	Corner	33.07	22.14		Corner	60.74	50.78
GTX-2	Central	35.63	30.78	MGR-1 (P1)	Central	68.33	55.63
	Lateral	28.62	30.41		Lateral	67.19	53.95
	Corner	26.19	28.70		Corner	64.64	53.52
GTX-2 (R)	Central	35.85	26.74	MGR-1 (P2)	Central	67.03	62.65
	Lateral	39.12	30.32		Lateral	79.36	65.01
	Corner	37.14	29.21		Corner	85.22	60.18

Notes: $J_{5\%}$ = secant tensile stiffness at 5% strain; The values of $J_{5\%}$ are mean values at each specimen location.

(MD and CMD considered) the statistical significance was the same for both T_{max} and $J_{5\%}$ variations (Tables 5, 7). In this sense, it should be noted that reduction factors are commonly applied only to T_{max} in design, although some statistically significant variations in $J_{5\%}$ were observed (Table 7). No statistically significant variation in tensile stiffness was observed in the tests with GTX, except for the tests with two reinforcement layers, where increases in $J_{5\%}$ were obtained along the cross-machine direction. These increases can be a consequence of variations in mass per unit area of GTX in combination with the influence of the impregnation of the geotextile by dust resulting from abrasion of the gravel particles during loading. The measurement of mass per unit area of GTX after the tests confirmed its impregnation by gravel dust. The impregnation of nonwoven geotextiles can increase their tensile stiffness, as observed by Mendes et al.

Table 7. Statistical significance of tensile stiffness variation.

Test	Direction	$J_{5\%-v}$ (kN/m)	$J_{5\%}$ (kN/m)	Significance
GTX-1	MD	31.54	30.30	NS
	CMD	23.84	30.09	NS
GTX-1 (R)	MD	31.54	32.61	NS
	CMD	23.84	23.00	NS
GTX-2	MD	31.54	30.15	NS
	CMD	23.84	29.96	S
GTX-2 (R)	MD	31.54	37.37	NS
	CMD	23.84	28.76	S
MGR-1	MD	80.20	66.51	S
	CMD	59.12	52.33	S
MGR-2	MD	80.20	62.32	S
	CMD	59.12	49.87	S
MGR-1 (P1)	MD	80.20	66.72	S
	CMD	59.12	54.37	S
MGR-1 (P2)	MD	80.20	77.20	NS
	CMD	59.12	62.61	NS

Notes: $J_{5\%-v}$ = secant tensile stiffness at 5% strain of virgin specimens; $J_{5\%}$ = secant tensile stiffness at 5% strain after the test; NS = not statistically significant with 95% confidence level; S = statistically significant with 95% confidence level.

(2007). On the other hand, significant reductions in tensile stiffness were noted in tests on MGR in both directions, except for test MGR-1(P2), where a heavier (900 g/m^2) protective geotextile layer was used between the reinforcement and the cap. This result shows that heavy nonwoven geotextiles would be required for an effective protection of the reinforcement layer. It can be noted in Figure 2a that tearing of the geogrid reinforcement took place despite the presence of a geotextile protective layer, which was also torn along the cap perimeter. The image in this figure suggests that a light geotextile may have been used for protection, and its failure corroborates what was observed in the present study regarding the need for heavier protective geotextile layers.

4. Reduction factors

The results of the tensile tests carried out on virgin and damage reinforcement specimens allow the evaluation of reduction factors for tensile strength and stiffness for the reinforcements tested. The reduction factors are defined as:

$$RF_T = \frac{T_{max-v}}{T_{max}} \quad (1)$$

$$RF_{J5\%} = \frac{J_{5\%-v}}{J_{5\%}} \quad (2)$$

Where RF_T = reduction factor for tensile strength, $RF_{J5\%}$ = reduction factor for tensile stiffness (secant, at 5% tensile strain), T_{max-v} = tensile strength of virgin reinforcement, T_{max} = tensile strength of damaged reinforcement, $J_{5\%-v}$ = tensile stiffness of virgin reinforcement and $J_{5\%}$ = tensile stiffness of damaged reinforcement.

The reduction factors for the different reinforcements tested are presented in Figure 7. In general, rather similar values of reduction factors were obtained in machine and cross-machine directions, ranging from 1.03 to 1.74 for RF_T and from 1.04 to 1.29 for $RF_{J5\%}$ (considering only values greater than 1), depending on the direction considered (MD or CMD). It should be pointed out that values of RF_T slightly greater than one could just be considered as one, since the statistical analysis did not show any relevant difference between tensile strengths of virgin and damaged specimens in these cases. However, values between 1.27 and 1.74 can be noted because of statistically relevant consequences of damages in the reinforcements after the tests. A few values of reduction factors smaller than one were observed in the case of geotextiles and this may be attributed to more significant variations of masses per unit area of the geotextiles at the locations where the specimens were collected in comparison with the average mass per unit area and, to some extent, the influence of geotextile impregnation by soil particles, as commented before.

Values of reduction factors commonly used in design to account for mechanical damages in geotextiles depend on the soil type, soil particle dimensions and shape, construction characteristics and geotextile mass per unit area (Jewell & Greenwood, 1988; Azambuja, 1994). In comparison with the gravel particle sizes in the present study, except for reinforcement GG, all the other reinforcements can be considered similar to geotextiles. For such cases, Figure 8a shows the variation of RF_T with reinforcement mass per unit area for tests with unprotected reinforcements. It can be noted that the lighter the reinforcement the greater the reduction factor obtained.

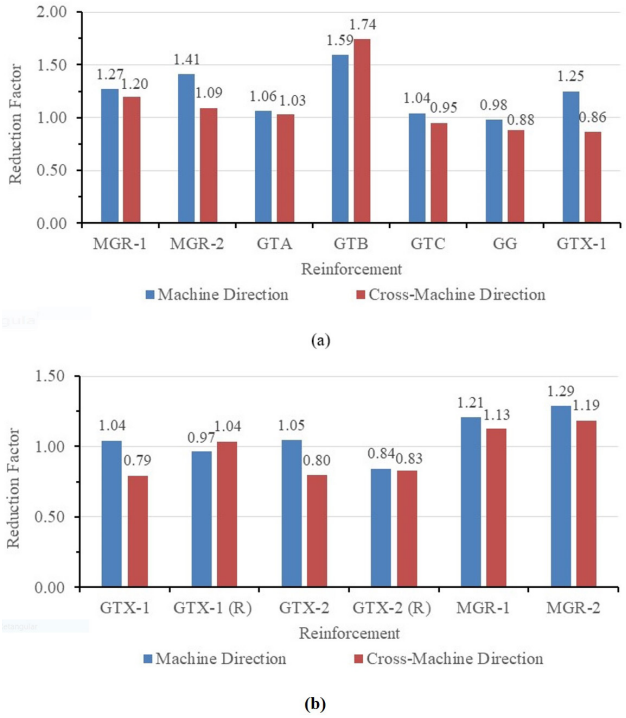

Figure 7. Reduction factors: (a) for tensile strength; (b) for tensile stiffness at 5% tensile strain.

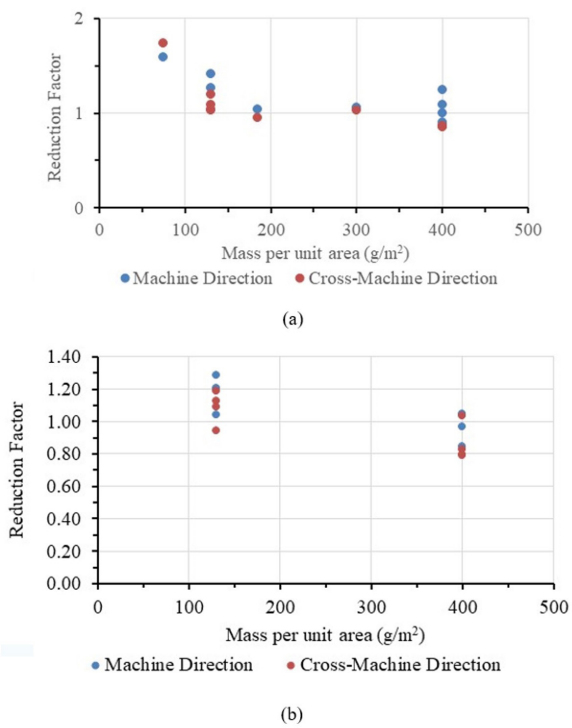

Figure 8. Reduction factors for tensile strength for geotextile like reinforcements versus mass per unit area: (a) RF_T; (b) $RF_{J5\%}$.

Despite some scatter, the reduction factor value tends to unity for masses per unit area greater than 150 g/m² for the scaling conditions of the tests. This suggests the need for much heavier geotextiles under prototype conditions. Despite the smaller number of test results, the same pattern of larger values of $RF_{J5\%}$ (1.04 to 1.29) for smaller masses per unit area can be noted in Figure 8b.

A similar trend of results can be observed when the reduction factors are plotted against the reinforcement tensile strength under virgin conditions ($T_{max\text{-}v}$) for unprotected reinforcements, as shown in Figure 9. There is also a trend of reduction RF_T and $RF_{J5\%}$ with increasing $T_{max\text{-}v}$. This behavior would be expected also for the nonwoven geotextiles tested, since the tensile strength of nonwoven, needle-punched, geotextiles is proportional to its mass per unit area.

The values of reduction factors back analyzed for reinforcement MGR with protective nonwoven geotextile layers are depicted in Figure 10 as a function of the protective layer mass per unit area (M_A). It can be noted that the geotextile protective layers were effective in reducing the effects of damages to MGR on its reinforcement strength (Figure 10a), bearing in mind that the differences between tensile strengths of damaged and virgin reinforcements did not have statistical significance (Table 5). However, that was not the case for the variations in tensile stiffness of MGR protected by the lighter geotextile (Figure 10b and Table 7). Despite the limited number of experimental data, the results obtained suggest that nonwoven geotextile protective layers heavier than (450 g/m², for the test scale) would be necessary. Under prototype conditions, a mass per unit area of the protective layer larger than 2000 g/m² would be recommended.

5. Mechanical damage index

It would be expected the effects of the mechanical damage to a tensioned and deformed geosynthetic reinforcement in contact with a mechanically aggressive rigid body edge to be a function of the geosynthetic surface characteristics, reinforcement tensile force, loading type (cyclic or static), inclination of the reinforcement with the horizontal direction at the reinforcement-edge contact (Figure 1a) and surface characteristics of the body edge. A dimensionless index to try to assess the level of reinforcement mechanical damage under such conditions can be expressed as:

$$MDI = \zeta_{es}\,\zeta_{rs}\,\zeta_{l}\,\frac{T}{T_{max-v}}\,\theta \qquad (3)$$

Where MDI = mechanical damage index, T = expected mobilized reinforcement tensile force (undamaged conditions), $T_{max\text{-}v}$ = reinforcement tensile strength under virgin conditions, θ = inclination (in radians) of the reinforcement with the horizontal direction at the reinforcement-edge contact point

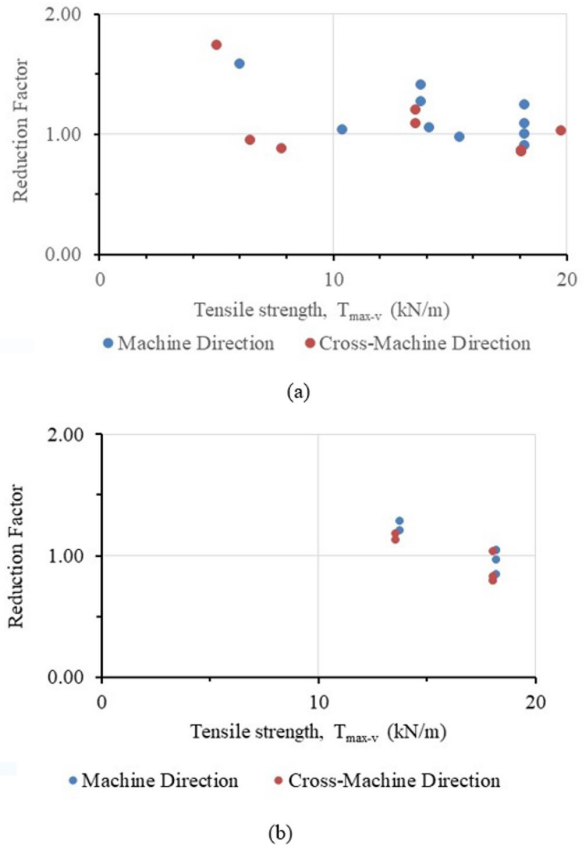

Figure 9. Reduction factors versus reinforcement tensile strength: (a) RF_T; (b) $RF_{J5\%}$.

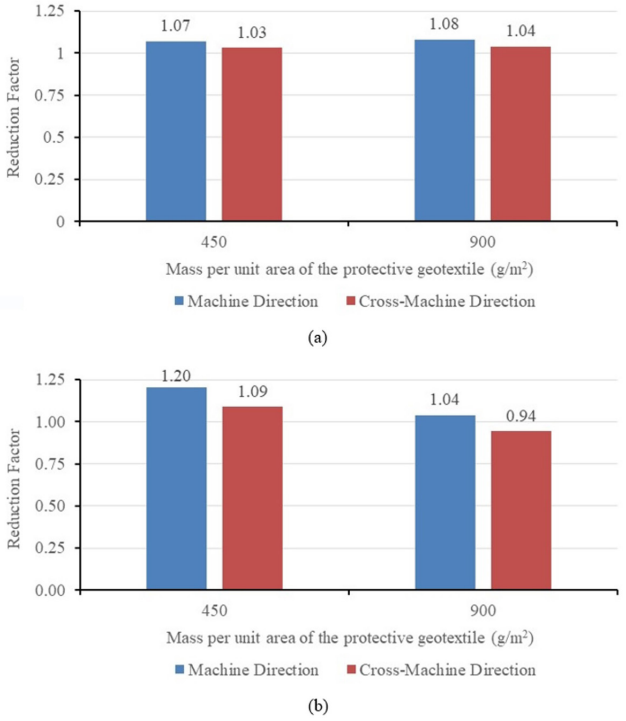

Figure 10. Reduction factors for geotextile protected reinforcement MGR: (a) RF_T; (b) $RF_{J5\%}$.

(Figure 1a), ζ_{es} = parameter to account for the aggressiveness of the body edge, ζ_l = parameter to consider the type of loading (=1 for static permanent loading and > 1 for cyclic loading) and ζ_{rs} = parameter to account for reinforcement surface characteristics (level of protection against damages).

The value of T can be obtained as a function of the expected reinforcement strain at the contact between reinforcement and cap edge and the tensile stiffness of the reinforcement. In analytical methods for geosynthetic reinforced piled embankments the value of T is commonly obtained as a function of the average reinforcement tensile strain, which is smaller than that value at the reinforcement-cap (or pile head) edge. The value of θ can be estimated based on the deformed shape of the reinforcement between caps. Analytical methods usually assume a parabolic or a catenary deformed shape for the reinforcement (BSI, 2010; Sloan 2011; Zhuang et al., 2014; van Eekelen, 2015, for instance). Fonseca et al. (2018) found little difference between predictions from these two shapes. The parameters ζ_{es}, ζ_{rs} and ζ_l should be equal or greater than one and determined from a large number of tests with different loading types and reinforcement and body edge surface conditions (smooth, rough, beveled etc.).

In the present study, the value of T used in Equation 3 was estimated based on the average reinforcement strain (ε) measured during the tests (Melchior Filho, 2022 and Fonseca & Palmeira, 2018) and the reinforcement tensile stiffness (J, $T = \varepsilon J$). For the sake of simplicity, in the present study the values of ζ_{es}, ζ_{rs} and ζ_{rs} are assumed as equal to 1. The angle θ (expressed in radians) was calculated by the following expression for a parabolic deformed shape of the reinforcement between caps:

$$\theta = tan^{-1}\left(\frac{4\delta_{max}}{s-a}\right) \quad (4)$$

Where δ_{max} = maximum reinforcement settlement between caps, s = centre to centre distance between caps and a = cap width.

Figure 11 shows the variation of reduction factors for tensile strength (RF_T) with MDI for unprotected and geotextile protected reinforcements from tests with a single layer of reinforcement. The results in this figure show RF_T values close to unity for MDI smaller than 0.08. Above this value a greater scatter of RF_T values can be noted with RF_T values between 1 and 1.74. Despite the rather limited number of results, larger values of RF_T are noted for larger MDI values. Values of the former very close to unity were obtained for the geotextile protected reinforcements and values of MDI

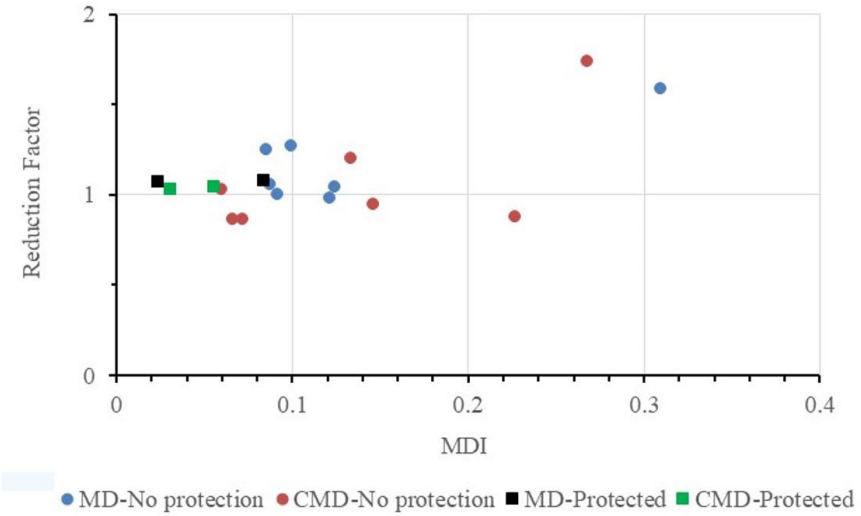

Figure 11. Reduction factor RF_T versus *MDI* for protected and unprotected reinforcements.

between 0.02 and 0.08. For the unprotected reinforcements, the results suggest that values of RF_T greater than 1.8 should be employed in designs where the reinforcement will be in contact with the cap or pile head for large values of *MDI*. Bearing in mind that monotonic loading was used in the tests carried out in this research, larger reduction factors would be necessary in case of cyclic loadings or for thinner fill layers.

6. Conclusions

This paper presented the results of an investigation aiming at quantifying the mechanical damage to geosynthetic reinforcements in reinforced piled embankment applications. The results and conclusions obtained may be extended to other situations of geosynthetic reinforcement in contact with mechanically aggressive rigid bodies. The main conclusions obtained in this investigation are summarized as follows.

Different intensities of damage were identified depending on the type and properties of the reinforcement tested and the damages influenced the values of reinforcement tensile strength and stiffness. Back analyzed reduction factors for the conditions of the tests varied between values slightly smaller than one and 1.74. The values smaller than one obtained are attributed to variations in mass per unit of the specimens in comparison to the average mass per unit area. In practice, reduction factor values must be greater than one. The larger the values of reinforcement mass per unit area of geotextile like reinforcements the smaller the back analyzed reduction factors for tensile strength and stiffness. These reduction factors also decreased with increasing tensile strength of the reinforcement under virgin conditions.

The protection of the reinforcement with a nonwoven geotextile layer was effective in reducing the mechanical damages, with back analyzed reduction factors for tensile strength smaller than 1.08 under the conditions of the tests. The statistical analysis showed no statistical relevance for the differences between tensile strengths of virgin and damaged reinforcements in tests with geotextile protection. However, in terms of prototype conditions, heavy nonwoven geotextiles will be required for an effective protection of the reinforcement against mechanical damages. The results obtained in the present work suggest that values of mass per unit area larger than 2000 g/m^2 under prototype conditions should be employed, particularly bearing in mind that the caps tested in the present work were smoother and with much better finishing than those typically found in the field.

The definition of a mechanical damage index was preliminarily introduced as a function of deformed geometry of the reinforcement, mobilized tensile force, tensile strength and parameters considering the mechanical aggressiveness of the cap, reinforcement surface characteristics and loading conditions. The ranges of possible values for the latter three parameters remain to be established based on a larger number of tests under different conditions. For the test conditions of the present work, a satisfactory correlation was observed between the mechanical damage index and the required reduction factor for reinforcement tensile strength.

The results obtained in this research highlight the importance of the use of appropriate reduction factors to account for the effects of mechanical damages of the reinforcement. This is particularly relevant in the case of repeated loading conditions, which can occur still during embankment construction, as well as for the durability and proper performance of the reinforcement during the project service life. Further research on appropriate values of reduction factors to be used in case of repeated loading is certainly necessary. Although the use of protective nonwoven geotextile layers between the reinforcement and the pile cap may be

effective, heavy geotextile layers are required. In this context, the installation of the reinforcement some distance above the cap is safer and even so appropriate reduction factors must be employed. Eventually, besides the use of reduction factors, the use of protective geotextile layers may also be recommendable depending on the project characteristics.

Acknowledgements

The authors are indebted to the University of Brasília and to the National Council for Scientific and Technological Development (CNPq) for their support for the research activities described in this paper.

Declaration of interest

The authors have no conflicts of interest to declare. All co-authors have observed and affirmed the contents of the paper and there is no financial interest to report.

Authors' contributions

Ennio Marques Palmeira: conceptualization, methodology, visualization, formal analysis, writing – review & editing. José Melchior Filho: conceptualization, supervision, data gathering, data validation, formal analysis, writing – original draft. Ewerton Clayton Alves Fonseca: conceptualization, supervision, data gathering, data validation, formal analysis, writing – review & editing.

List of symbols and abbreviations

a	Pile cap width (mm)
C_u	Soil uniformity coefficient (dimensionless)
D_n	Diameter for which n (%) in mass of the remaining particles have smaller diameters (mm)
G_s	Soil particle specific gravity (dimensionless)
$J_{5\%}$	Secant tensile stiffness at 5% strain of damaged reinforcement (kN/m)
$J_{5\%\text{-}v}$	Secant tensile stiffness at 5% strain of virgin reinforcement (kN/m)
M_A	Geosynthetic mass per unit area (g/m^2)
T	Mobilized reinforcement tensile load (kN/m)
T_{max}	Tensile strength of damaged reinforcement (kN/m)
$T_{max\text{-}v}$ (kN/m)	Tensile strength of virgin (undamaged) reinforcement
RF_T	Reduction factor for tensile strength (dimensionless)
$RF_{J5\%}$	Reduction factor for tensile stiffness at 5% strain (dimensionless)
s	Pile spacing (mm)
δ_{max}	Maximum settlement of the reinforcement between caps (mm)
$\gamma_{d,}$	Dry soil unit weight (kN/m^3)
ϕ'	Soil friction angle (degrees)
θ	Inclination of the reinforcement to the horizontal at the contact with the cap (radians)
ζ_l	Parameter for loading type (dimensionless)
ζ_{es}	Parameter for cap edge surface (dimensionless)
ζ_{rs}	Parameter for reinforcement surface (dimensionless)

References

ABNT NBR 6458. (2016). *Gravel grains retained on the 4,8 mm mesh sieve – Determination of the bulk specific gravity, apparent specific gravity and water absorption.* ABNT - Associação Brasileira de Normas Técnicas, Rio de Janeiro, RJ (in Portuguese).

ABNT NBR 7181. (2016). *Soil – Grain Size Analysis.* ABNT - Associação Brasileira de Normas Técnicas, Rio de Janeiro, RJ (in Portuguese).

Abusharar, S.W., Zheng, J.-J., Chen, B.-G., & Yin, J.-H. (2009). A simplified method for analysis of piled embankment reinforced with geosynthetics. *Geotextiles and Geomembranes*, 27(1), 39-52. http://dx.doi.org/10.1016/j.geotexmem.2008.05.002.

Almeida, M.S.S., & Marques, M.E.S. (2011). Construction methods in Brazilian extremely soft soils. In *Proceedings of the Pan-Am CGS Geotechnical Conference* (16 p.). Toronto, Ontario, Canada.

Al-Taie, E.T., Al-Kalali, H.H., & Fattah, M.Y. (2019). Evaluation of settlement and bearing capacity of embankment on soft soil with reinforced geogrids. *International Journal of Engineering Research & Technology (Ahmedabad)*, 8(6), 99-103. http://dx.doi.org/10.17577/IJERTV8IS060044.

Austin, R. (1997). The effect of installation activities and fire exposure on geogrid performance. *Geotextiles and Geomembranes*, 15(4-6), 367-376. http://dx.doi.org/10.1016/S0266-1144(98)80009-5.

ASTM D6637. (2015). *Standard test method for determining tensile properties of geogrids by the single or multi-rib tensile method*. ASTM International, West Conshohocken, PA.

ASTM D4595. (2017). *Standard test method for tensile properties of geotextiles by the wide-width strip method*. ASTM International, West Conshohocken, PA.

Azambuja, E. (1994). *Investigação do dano mecânico em geotêxteis não tecidos* [Masters dissertation]. Universidade Federal do Rio Grande do Sul.

Bathurst, R.J., & Miyata, Y. (2015). Reliability-based analysis of combined installation damage and creep for the tensile rupture limit state of geogrid reinforcement in Japan. *Soil and Foundation*, 55(2), 437-446. http://dx.doi.org/10.1016/j.sandf.2015.02.017.

BSI BS 8006. (2010). *Code of practice for strengthened/reinforced soils and other fills*. British Standards Institution, United Kingdom.

Cho, S.D., Lee, K.W., Cazzuffi, D.A., & Jeon, H.Y. (2006). Evaluation of combination effects of installation damage and creep behavior on long-term design strength of

geogrids. *Polymer Testing*, 25(6), 819-828. http://dx.doi.org/10.1016/j.polymertesting.2006.04.007.

EBGEO. (2011). *Recommendations for design and analysis of earth structures using geosynthetic reinforcements - EBGEO*. Germany: EBGEO.

Fattah, M.Y., Zabar, B.S., & Hassan, H.A. (2015). Soil arching analysis in embankments on soft clays reinforced by stone columns. *Structural Engineering and Mechanics*, 56(4), 507-534. http://dx.doi.org/10.12989/sem.2015.56.4.507.

Fattah, M.Y., Mohammed, H.A., & Hassan, H.A. (2016a). Load transfer and arching analysis in reinforced embankment. *Structures and Buildings, Proceedings - Institution of Civil Engineers*, 169(11), 797-808. http://dx.doi.org/10.1680/jstbu.15.00046.

Fattah, M.Y., Zabar, B.S., & Hassan, H.A. (2016b). Experimental analysis of embankment on ordinary and encased stone columns. *International Journal of Geomechanics*, 16(4), 04015102. http://dx.doi.org/10.1061/(ASCE)GM.1943-5622.0000579.

Federal Highway Administration – FHWA. (2017). *Ground modification methods reference manual* (Vol. 2, No. FHWA-NHI-16-028, 542 p.). Washington: Federal Highway Administration, US Department of Transportation.

Filz, G.M., & Smith, M.E. (2006). *Design of bridging layers in geosynthetic-reinforced column-supported embankments* (46 p.). Charlottesville, VA, USA: Virginia Transportation Research Council.

Filz, G.M., & Smith, M.E. (2007). Net vertical loads on geosynthetics reinforcement in column-supported embankments. In *Proceedings of the Soil Improvement* (Geotechnical Special Publication, No. 172). Reston, VA, USA: Geo-Institute of ASCE. http://dx.doi.org/10.1061/40916(235)1.

Fleury, M.P., Santos, E.C.G., Lins da Silva, J., & Palmeira, E.M. (2019). Geogrid installation damage caused by recycled construction and demolition waste. *Geosynthetics International*, 26(6), 641-656. http://dx.doi.org/10.1680/jgein.19.00050.

Fonseca, E.C.A. (2017). *Estudo experimental do comportamento de aterros estaqueados reforçados com geossintéticos* [PhD thesis]. Departamento de Engenharia Civil e Ambiental, Universidade de Brasília.

Fonseca, E.C.A., & Palmeira, E.M. (2018). Evaluation of the accuracy of design methods for geosynthetic reinforced piled embankments. *Canadian Geotechnical Journal*, 56(6), 761-773. http://dx.doi.org/10.1139/cgj-2018-0071.

Fonseca, E.C.A., Palmeira, E.M., & Barrantes, M.V. (2018). Load and deformation mechanisms in geosynthetic-reinforced piled embankments. *International Journal of Geosynthetics and Ground Engineering*, 4(32), 1-12. http://dx.doi.org/10.1007/s40891-018-0150-x.

Gonzalez-Torre, I., Calzada-Perez, M.A., Vega-Zamanillo, A., & Castro-Fresno, D. (2014). Damage evaluation during installation of geosynthetics used in asphalt pavements. *Geosynthetics International*, 21(6), 377-386. http://dx.doi.org/10.1680/gein.14.00025.

Hsieh, C. W., & Wu, J. H. (2001). Installation survivability of flexible geogrids in various pavement subgrade materials. *Transportation Research Record: Journal of the Transportation Research Board*, 1772(1), 190-196. http://dx.doi.org/10.3141/1772-23.

Huang, C.C. (2006). Laboratory simulation of installation damage of a geogrid. *Geosynthetics International*, 13(3), 120-132. http://dx.doi.org/10.1680/gein.2006.13.3.120.

Hufenus, R., Ruegget, R., & Flum, D. (2002). Geosynthetics for reinforcement – resistance to damage during installation. In D. Cazzuffi, J. Greenwood, M. Heibaum, D. Leshchinsky & F. Tatsuoka (Eds.), *Proceedings of the 7th International Conference on Geosynthetics* (Vol. 2, pp. 1387-1390). USA: International Geosynthetics Society (IGS).

Jewell, R.A., & Greenwood, J.H. (1988). Long term strength and safety in steep soil slopes reinforced by polymer materials. *Geotextiles and Geomembranes*, 7(1-2), 81-118. http://dx.doi.org/10.1016/0266-1144(88)90020-9.

Low, B.K., Tang, S.K., & Choa, V. (1994). Arching in piled embankments. *Journal of Geotechnical Engineering*, 120(11), 1917-1938. http://dx.doi.org/10.1061/(ASCE)0733-9410(1994)120:11(1917).

Melchior Filho, J. (2022). *Estudo da interação solo-reforço-geossintético em aterros estaqueados por meio de ensaios de grandes dimensões* [PhD thesis]. University of Brasilia (in progress).

Mendes, M.J.A., Palmeira, E.M., & Matheus, E. (2007). Some factors affecting the in-soil load–strain behaviour of virgin and damaged nonwoven geotextiles. *Geosynthetics International*, 14(1), 39-50. http://dx.doi.org/10.1680/gein.2007.14.1.39.

Pinho-Lopes, M., Paula, A.M., & Lopes, M.L. (2018). Long-term response and design of two geosynthetics: effect of field installation damage. *Geosynthetics International*, 25(1), 98-117. http://dx.doi.org/10.1680/jgein.17.00036.

Richardson, G. (1998). Field evaluation of geosynthetic survivability in aggregate road base. *Geotechnical Fabrics Report*, 16(7), 34-38.

Rosete, A., Mendonça Lopes, P., Pinho-Lopes, M., & Lopes, M.L. (2013). Tensile and hydraulic properties of geosynthetics after mechanical damage and abrasion laboratory tests. *Geosynthetics International*, 20(5), 358-374. http://dx.doi.org/10.1680/gein.13.00022.

Russel, D., & Pierpoint, N. (1997). *An assessment of design methods for piled embankments* (Ground Engineering, Vol. 30, No. 10, pp. 39-44). London, United Kingdom: EMAP Construct Limited.

Sloan, J.A. (2011). *Column-supported embankments: full-scale tests and design recommendations* [PhD thesis]. Virginia Polytechnic Institute and State University.

Sloan, J.A., Filz, G.M., & Collin, J.G. (2011). A generalized formulation of the adapted Terzaghi method of arching in column-supported embankments. In J. Han & and D.

E. Alzamora (Eds.), *Proceedings of the Geo-Frontiers: Advances in Geotechnical Engineering* (Geotechnical Special Publication, No. 211, pp. 798-805). Reston, VA, USA: Geo-Institute of ASCE. http://dx.doi.org/10.1061/41165(397)82.

van Eekelen, S.J.M. (2015). *Basal reinforced piled embankments* [PhD thesis]. Technical University of Delft.

van Eekelen, S.J.M. (2016). The 2016-update of the dutch design guideline for basal reinforced piled embankments. *Procedia Engineering*, 143, 582-589. http://dx.doi.org/10.1016/j.proeng.2016.06.077.

Yoo, H., Jeon, H.Y., & Chang, Y.C. (2009). Evaluation of engineering properties of geogrids for soil retaining walls. *Textile Research Journal*, 80(2), 184-192. http://dx.doi.org/10.1177/0040517508093442.

Zhuang, Y., Wang, K.Y., & Liu, H.L. (2014). A simplified model to analyze the reinforced piled embankments. *Geotextiles and Geomembranes*, 42(2), 154-165. http://dx.doi.org/10.1016/j.geotexmem.2014.01.002.